PREPARATION, CHARACTERIZATION, ANTIBACTERIAL EVALUATION, LASER ACTIVITY, MOLECULAR DOCKING, AND LIQUID CRYSTALLINITY STUDIES OF NEW TETRAZOLE DERIVATIVES

Nour A. Yassin*, Fawzi H. Jumaa

Department of Chemistry, College of Education for Women, Tikrit University
**e-mail: noor.yasseen23@st.tu.edu.iq*

Received 17.05.2025
Accepted 15.07.2025

Abstract: *In this study, the sublimation technique was employed to react equimolar amounts of Schiff base derivatives with sodium azide in the presence of DMSO as a solvent for 21–22 hours. The result is a synthesis of five-membered tetrazole derivatives. Physical and spectroscopic techniques, including infrared, proton and carbon nuclear magnetic resonance, validated the compounds' structures, and UV-Vis spectroscopy. Thin-layer chromatography (TLC) was used to monitor the reaction progress and identify the melting points and purities. Two bacterial isolates, one Gram-positive (Staphylococcus aureus) and one Gram-negative (Escherichia coli), were examined to determine how certain chemicals they produced affected their growth. Some of the produced compounds had good inhibitory action against the tested microorganisms. At a dosage of 0.1 mg/ml and an inhibition diameter of 1.7 cm, compound N_6 exhibited the maximum inhibition, surpassing the antibiotic's efficiency. With an inhibition diameter of 3.6 cm at a dose of 0.1 mg/ml, compound N_{10} had the strongest inhibitory action against Escherichia coli bacteria, surpassing the antibiotic in all experiments. The antibiotic ciprofloxacin was employed as a control. Furthermore, the prepared compounds were exposed to neodymium nano-laser radiation. The compounds demonstrated high stability toward the radiation. Molecular modelling was performed using the AUTODOCK software package for N_6 against S. aureus and N_{10} against E. coli. It appears that tetrazole is linked via the NH group with amino acid residue B: GLY:114, forming hydrogen bonds with an affinity value of (-9.9 kcal/mol) and a conformational value of RMSD.i.b (4.721) and RMSD.u.b (8.679). The textures of some of the prepared compounds [N6, N8] were studied using a polarizing microscope.*
Keywords: *Tetrazoles, bacterial bioactivity, laser, molecular docking, liquid crystalline*

1. Introduction

Given the significant role of heterocyclic compounds in pharmacology, this class of substances has attracted considerable attention in recent years [1, 2]. Nitrogen-containing heterocycles, in particular, represent a highly versatile category of molecules with wide-ranging applications in industrial chemistry, synthetic organic chemistry, and medicinal chemistry [3]. Moreover, the growing emphasis on sustainability has encouraged chemists to develop more environmentally friendly and efficient synthetic methodologies. Among these compounds, tetrazoles occupy a prominent position as five-membered heterocycles composed of four nitrogen atoms and one carbon atom. They exist in three possible isomeric forms:

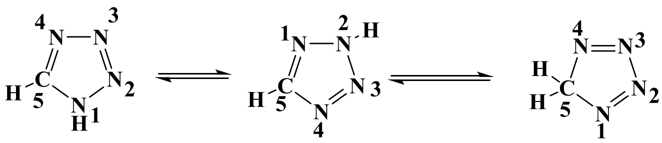

1*H*-tetrazole 2*H*-tetrazole 5*H*-tetrazole

Although research in heterocyclic chemistry has advanced considerably, much of the applied focus has centered on the diverse applications of tetrazolyl-containing heterocyclic compounds. Tetrazoles were first synthesized by Bladin in 1855, and since then, the number of studies devoted to their synthesis and applications has steadily increased [4]. Owing to their high nitrogen content, tetrazoles possess a higher heat of formation, resulting from an elevated ratio of nitrogen–nitrogen to carbon–nitrogen bonds. Furthermore, their low C–H bond content imparts exceptional resistance to shock, impact, and electrostatic discharge [5].

The tetrazole ring plays a crucial role in the design of numerous bioactive molecules exhibiting activity against bacterial and viral pathogens [6]. In medicinal chemistry, tetrazoles are often employed as bioisosteric substitutes for carboxylic acid groups or as structural spacers [7]. Beyond pharmaceutical applications, tetrazoles are valuable in the development of energetic materials and serve as key intermediates in the synthesis of various heterocyclic systems. Their five-membered ring framework offers an ideal platform for constructing functionalized molecular architectures. Moreover, tetrazole-containing compounds constitute an important class of drug carriers, contributing to the development of potential anticancer agents. A variety of promising materials—both coordination complexes and naturally derived compounds—have been reported to contain tetrazole moieties [8]. Previous investigations have also demonstrated that the tetrazole ring exhibits notable antibacterial activity [9].

The present study aims to synthesize a series of tetrazole derivatives using dimethyl sulfoxide (DMSO) as a solvent and to evaluate their antibacterial activity against *Staphylococcus aureus* and *Escherichia coli*. Additionally, the work explores several physicochemical and functional aspects, including laser radiation stability, molecular docking of the most active compounds and liquid-crystalline behavior examined via polarizing microscopy.

2. Experimental part

2.1. Material: Aldrich, Fluka, and BDH manufacture; all the compounds without refining.

2.2. Synthesis of tetrazole derivatives [N_{10}-N_6]. 0.0006 mole of Schiff bases [N_5-N_1] were added to 25 ml of dimethyl sulfoxide with 0.15 g (0.0018 mole) of sodium azide in 15 ml of the same solvent, and the mixture was stirred for 21-22 h. TLC monitored the completion of the reaction [10, 11]. The mixture's temperature was lowered, filtered, and washed with cold water. It was then recrystallized with tetrahydrofuran and dried at 50 °C, as in Table 1.

Table 1. Some physical properties of tetrazole compounds [N_6-N10]

Comp. No.	R	Molecular Formula/ M.Wt g/mol	Color	M.P. (^{0}C)	R.T hour	R_f	Yield (%)
***N_6**	OH	$C_{45}H_{36}N_{12}O_3$ 792	Black	215-217	21	0.93	80
N_7	Br	$C_{45}H_{33}N_{12}Br_3$ 978	Yellow	145-147	21	0.95	75
***N_8**	NO_2	$C_{45}H_{33}N_{15}O_6$ 879	Brown	169-171	22	0.91	86
N_9	Cl	$C_{45}H_{33}N_{12}Cl_3$ 848	Drak Brown	89-91	22	0.83	78
N_{10}	CH_3O	$C_{48}H_{42}N_{12}O_3$ 835	Light Green	95-97	22	0.90	89

*Note: Compounds marked with an asterisk have had their liquid crystalline phases studied.

2.3. Evaluation of bacterial bioactivity. Serial twofold dilutions of normal saline determined the potency of the studied compounds. Potency is the reciprocal of the highest dilution that resulted in an apparent growth inhibition zone and is expressed in cm. The method for measuring potency was Wells' method. Test bacteria were cultured in liquid nutrient medium at 37°C for 2 hours. 0.1 ml of the previous culture was transferred to a plate using a diffuser, and a diffuser was placed on the surface of the plate [12, 13]. The plate was then incubated at 37°C for 10 minutes. Half of the compounds were then serially prepared for each compound at three different dilutions (0.1, 0.01, and 0.001 mg/ml). Wells' etching was performed on the plates, and 0.2 ml of each dilution was placed in each hole. The plates were incubated at 37°C for 24 hours, and the results were recorded to determine whether there was a growth inhibitory effect around each hole [14, 15].

2.4. Study of the effect of laser radiation on some prepared compounds. A neodymium nano-laser system (Nd: YAG laser) with a wavelength of 808 nm and a frequency of 5 Hz was applied to the compounds [N_6, N_7, N_8, N_9, and N_{10}]. A concave quartz lens with a focal length of 100 mm was used to impact the laser radiation on the samples vertically, and the laser waves were fired for 40 seconds at a distance of 10 cm between the laser source and the samples [16].

2.5. Study of the molecular docking of some prepared compounds. All molecular modeling was performed using Autodock. Structural formulas were generated using ChemDraw Professional version 16.0, converted to low-energy-barrier 3D structures using Chem3D version 16.0, and saved as .pdb files. The tertiary structures of proteins with PDB:ID: 3jzf and PDB:ID: 4dq2 were obtained from the Protein Data Bank (PDB) website. The ligand and protein were converted from .pdb to .pdbqt using AutoDockTools version 1.5.6 and saved in a new molecular modeling folder. Discovery Studio 2020 Client was used to visualize the 2D and 3D configurations of the ligand-protein interaction. RMSD values, hydrogen bonds, and correlations with the amino acid sequences of the protein were also calculated [17].

2.6. Study of liquid crystalline phases using a polarized light microscope. The structures of some of the prepared compounds [N_6, N_8] were observed using a Meiji-Evolution hot-plume polarizing microscope, an E-PLAN 10x/0.25 160/0.17 lens, an electronic thermometer to monitor temperature changes, and a 38 mp FHD V6 camera with 20x magnification. A thin layer of each studied material was formed, and the samples were then examined using a magnifying glass and a thermal camera that automatically records temperature changes. The patterns of the studied materials were documented [18].

3. Results and discussion

Tetrazole derivatives (N_6-N_{10}) were generated by combining three equivalent amounts of prepared Schiff base derivatives (N_1-N_5) with one equivalent of sodium azide in the presence of DMSO as a solvent, as shown in the following scheme:

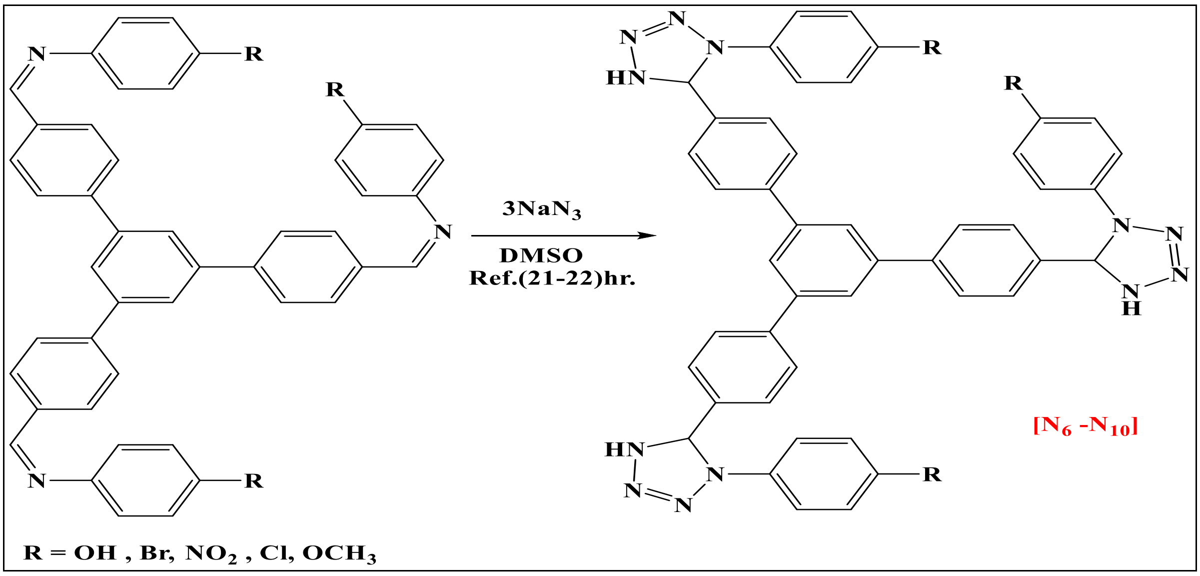

Scheme 1. Path of the Ready compounds (N_6-N_{10})

3.1. Characterization of Tetrazole derivatives (N_6-N_{10}). While studying the UV-vis spectrum of [N_6-N_{10}] compounds in absolute ethanol as a solvent at concentrations of [10^{-5} - 10^{-4}]' short wavelengths (λ_{max}) appeared at (253-272) nm, which are attributed to the ($^*\pi\leftarrow\pi$) transition, while long wavelengths (λ_{max}) were observed at (338-286) nm, which are attributed to the ($^*\pi\leftarrow$n) transition.

When studying the infrared spectrum of the prepared compounds [N_6-N_{10}], in the prepared Schiff base compounds [N_1-N_5], it was observed that the azomethine group (C=N) stretching band that had appeared in the range (1618-1612) cm^{-1} had vanished. A medium band had appeared in the range (3272-3423) cm^{-1}, which was caused by the stretching of the (N-H) group in the tetrazole ring. Additionally, an absorption band had appeared in the range (3043-3072) cm^{-1}, which was caused by the stretching of the aromatic (C-H) bond, and an absorption band in the range (2848-2945) cm^{-1}, which was caused by the stretching of the aliphatic (CH) bond.in addition to the appearance of two bands in the range (1508-1461) cm^{-1} and (1583-1570) cm^{-1}, which are due to the vibration of the aromatic (C=C) bond, and the appearance of medium bands in the range (1413-1396) cm^{-1} belong to the (N=N) group, which was attributed to the formed tetrazole ring. These bands were close to what is found in the literature. Along with the emergence of medium bands in the range (1413-1396) cm^{-1} that belong to the (N=N) group, which was ascribed to the created tetrazole ring, The stretching of the (C-N) bond was identified as the cause of additional bands in the (1205-1236) cm^{-1} region seen in FT-IR spectra. These bands closely resembled those in the literature [19, 20] (Table 1, Fig.s 1 and 2).

Table 2. FT-IR absoption results for Tetrazole derivatives (N_6-N_{10})

Comp. No.	**λ_1 max nm** **λ_2 max nm**	**R**	**IR (KBr) cm^{-1}**					
			νN-H	**νC-H Arom.**	**νC-H Aliph.**	**νC=C Arom.**	**νC-N νN=N**	**Others**
N_6	253 338	OH	3302	3072	2872	1581 1478	1216 1413	ν (OH) 3487
N_7	256 361	Br	3272	3057	2869	1578 1469	1221 1409	ν (C-Br) 548
N_8	261 347	NO_2	3279	3043	2945	1583 1481	1205 1396	ν(NO_2) *asy*. (1521) *sym*. (1317)
N_9	272 364	Cl	3423	3064	2883	1570 1508	1236 1406	ν (C-Cl) 750
N_{10}	268 386	OCH_3	3285	3058	2935 2848	1575 1461	1214 1412	ν (C-O-C) *asy*. (1364) *sym*. (1249)

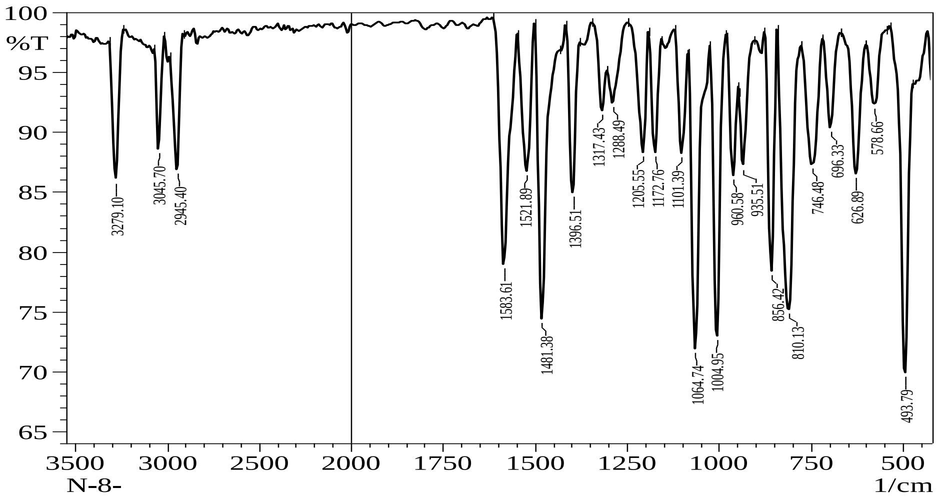

Fig. 1. FT-IR spectrum for compound [N_8]

When studying the ^{1}H-NMR spectrum of the compound [N_7] in the solvent (DMSO-d6), multiple signals were observed in the range (7.14-7.91) ppm, and this signal was attributed to the protons of the aromatic rings. One signal was observed at the chemical shift (5.27) ppm, which was attributed to the (CH) group in the tetrazole ring. One signal was observed at the chemical shift (4.17) ppm, which was attributed to the (NH) group. A signal was observed at the chemical shift (2.50) ppm, which was attributed to the protons of the solvent (DMSO-d6) (Fig. 3).

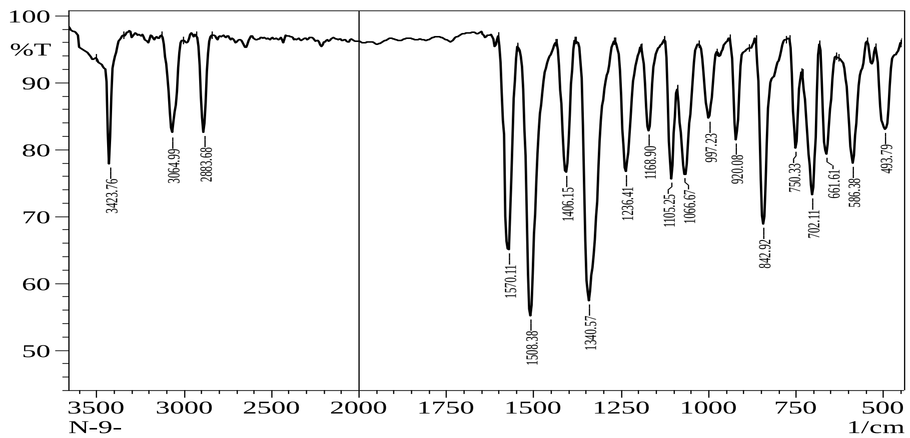

Fig. 2. FT-IR spectrum for compound [N_9]

When studying the ^{13}C-NMR spectrum of the compound [N_7] in the solvent (DMSO-d6), multiple signals were observed at chemical shifts (144.64, 138.84, 141.46, 136.06, 134.08, 132.53, 128.93, 127.85, 125.52, 122.94) ppm, which were attributed to the carbon atoms in the aromatic ring, as well as the appearance of a signal at chemical shift (88.79) ppm, which was attributed to the carbon of the (CH) group in the tetrazole ring, and the appearance of a signal at chemical shift (39.12-40.79) ppm, which was attributed to the carbon of the solvent (DMSO-d6) (Fig. 4).

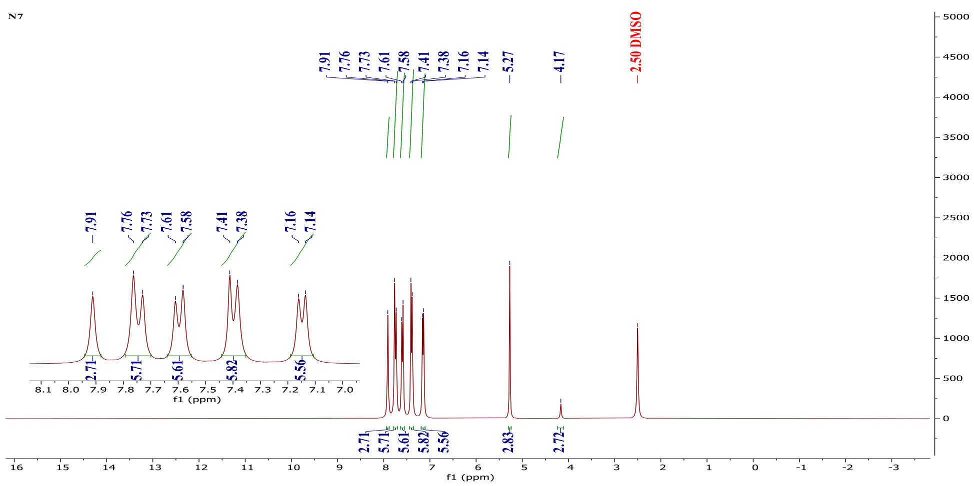

Fig. 3. ^{1}H-NMR spectrum for compound [N_7]

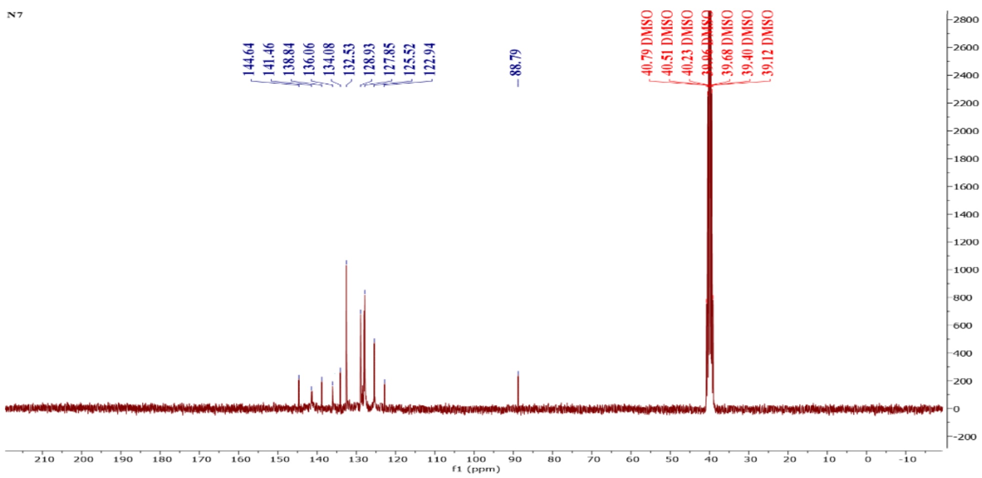

Fig. 4. ^{13}C-NMR spectrum for compound [N_7]

3.2. Bacterial susceptibility to prepared compounds. Using the antibiotic *Ciprofloxacin* as a reference sample, the sensitivity of the inhibitory compounds was evaluated against two bacterial species, *Escherichia coli* and *Staphylococcus aureus*. With an inhibition diameter of 3.6 cm at a dose of 0.1 mg/ml, compound N_{10} had the strongest inhibitory action against *Escherichia coli* bacteria, surpassing the antibiotic in all experiments. The diameter of inhibition was measured in centimeters. With an inhibition diameter of 1.9 cm and a dose of 0.001 mg/ml, the same chemical, N_{10}, demonstrated the greatest inhibition of *Staphylococcus aureus* bacteria [21-23]. At a dosage of 0.1 mg/ml and an inhibition diameter of 1.7 cm, compound N_6 exhibited the maximum inhibition, surpassing the antibiotic's efficiency. This indicates the possibility of using them as antibiotics in the future [24-28]. As for the rest of the compounds' effectiveness against bacteria, it varied, as shown in Table 2, Scheme 2, and Fig. s 5 and 6.

Table 2. Antibacterial activity of the synthesized compounds (inhibition zone in cm)

Comp No.	E.coli mg/ml			Staph. aureus mg/ml		
	0.1	**0.01**	**0.001**	**0.1**	**0.01**	**0.001**
N_6	1.0	2.1	0.5	1.7	1.5	1.5
N_7	1.0	1.5	2.0	0.5	0.5	1.0
N_8	0.8	1.0	1.5	1.5	1.0	1.5
N_9	0.6	1.0	1.0	1.0	1.3	1.7
N_{10}	3.6	1.8	1.0	1.0	0.4	1.9
Ciprofloxacin	2.0	1.5	1.3	1.5	1.5	1.2

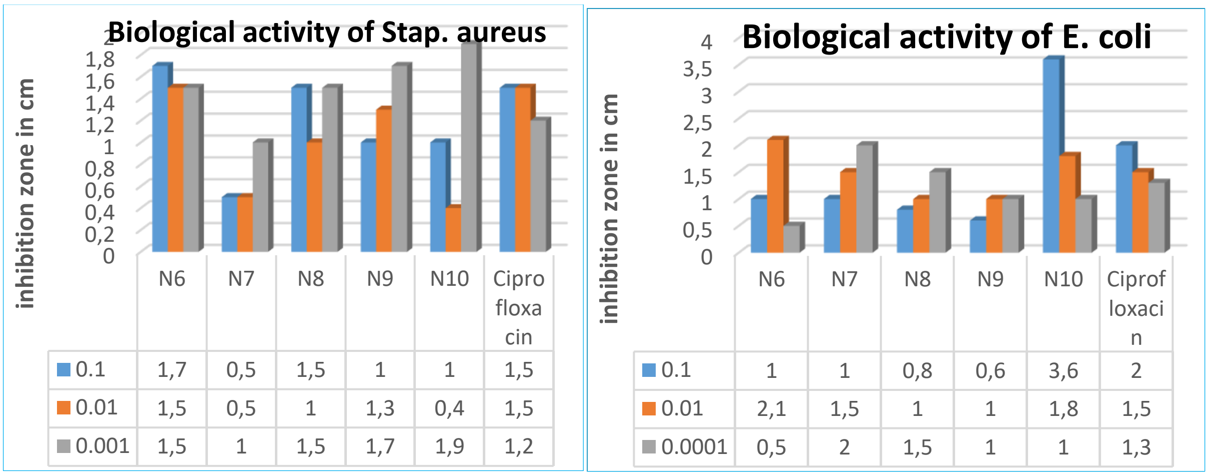

Scheme 2. Inhibitory activity of [N6-N10] for *Staf. aureus and E. coli*

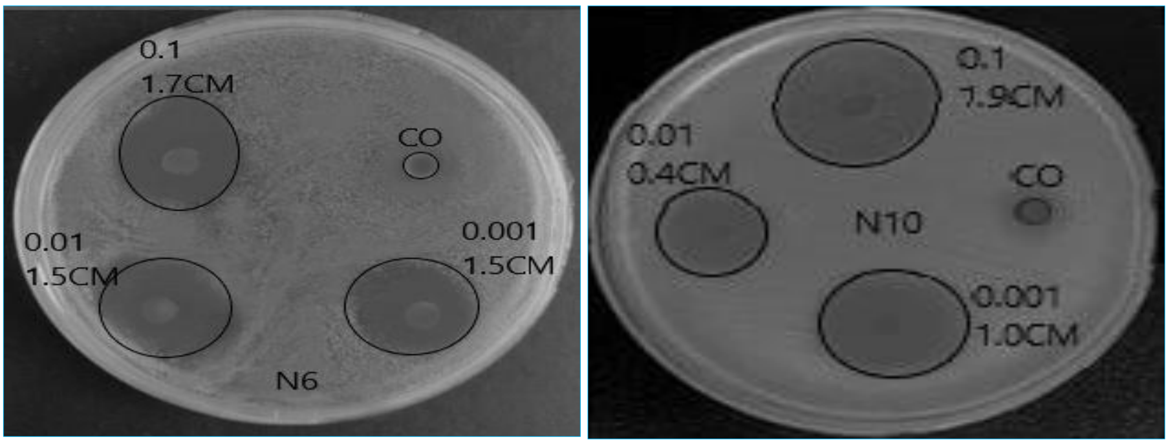

Fig. 5. Inhibitory activity of the two compounds [N_6, N_{10}] against *Staph. aureus*

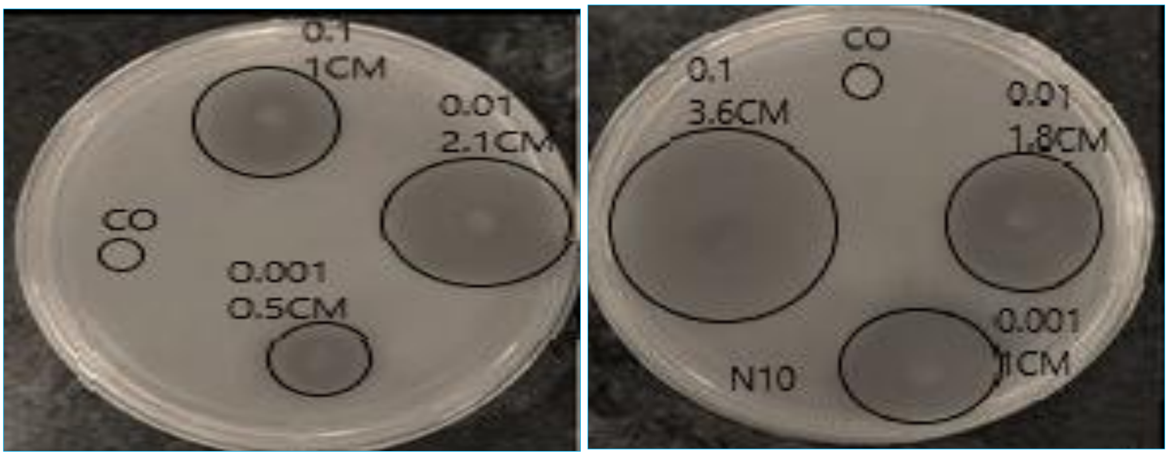

Fig. 6. Inhibitory activity of the two compounds [N_6, N_{10}] against *E.coli*

3.3. Results of measuring the laser activity of some prepared compounds. By measuring the melting point before and after laser bombardment, it was found that the studied compounds were unaffected by the laser bombardment process. Neither their color nor their melting point changed. After laser exposure, the measured values remained unchanged. It is clear that laser radiation does not affect the compounds under laser bombardment conditions [29-31], as shown in Table 3.

Table 3. Results of measuring the laser activity of some prepared compounds

Comp. No.	Before Irradiation		After Irradiation	
	M.P. ^0C	Color	M.P. ^0C	Color
N_{21}	215-217	Black	215-217	Black
N_{22}	145-147	Yellow	145-147	Yellow
N_{23}	169-171	Brown	169-171	Brown
N_{24}	89-91	Drak Brown	89-91	Drak Brown
N_{25}	95-97	Light Green	95-97	Light Green

3.4. Molecular docking results. Molecular modelling of compound N6, which showed high inhibitory activity against S. aureus, was performed. The biotin protein ligase enzyme, which plays a prominent role in the metabolism of lipids, proteins, and carbohydrates, was selected. Its inhibition contributes to reducing or preventing the growth of this bacterium. The enzyme with PDB ID: 4dq2 was selected, and the grid box of this protein was determined using AutoDockTools 1.5.6 with dimensions (45, 45, 45, 45) (X, Y, Z) and position coordinates (51.15, 19.715, 22.1) (X, Y, Z).

The derivative N6 was bound to the binding site of the enzyme at a docking score of -10.4 Kcal/mol and at a conformational value of RMSD.i.b(5.193) and RMSD.u.b(10.388). The two- and three-dimensional imaging sections showed the presence of three hydrogen bonds between the amino acid residues A:SER:93 and the NH group in the tetrazole ring at a distance of 2.51 Å. These relatively short distances reflect the strength of these bonds and their role in stabilizing the compound inside the active site, and two hydrogen bonds between the amino acid residues A:THR:94 and the N=N group at a distance of 2.82 Å and the NH group in the tetrazole ring at a distance of 3.07 Å, in addition to some other bonds, as shown in Fig. 7 and Table 4.

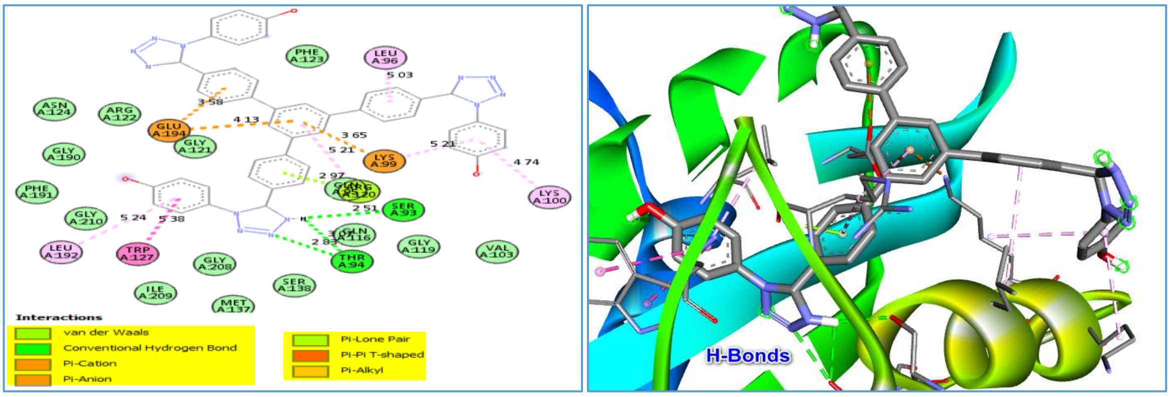

Fig. 7. 2D and 3D representation of N_6 with the binding site of the protein (PDB ID: 4dq2)

Biotin carboxylase was selected to perform the molecular docking of compound N_{10}, which showed high inhibitory activity against E. coli, which is of great importance in the metabolism of lipids, proteins and carbohydrates, and therefore, stopping the work of this enzyme contributes to weakening or preventing the growth of this bacterium. The enzyme (PDB: ID: 3jzf) was selected, and the grid box of this protein was determined using AutoDockTools: 1.5.6, and its dimensions were (40, 40, 40, 40) (X, Y, Z), and its location parameters were (40, 40, 40) (X, Y, Z) [32].

The derivative N_{10} was bound to the enzyme binding site at a docking score of (-9.9 Kcal/mol) and at a conformational value of RMSD.i.b(4.721), RMSD.u.b(8.679). The two-dimensional and three-dimensional imaging sections showed the presence of three hydrogen bonds between the amino acid residues B:GLY:114 and the NH group in the tetrazole ring at a distance of 2.39 Å. These relatively short distances reflect the strength of these bonds and their role in stabilizing the compound inside the active site: a hydrogen bond between B:ARG:338 and the OCH_3 group at a distance of 3.35 Å, and a hydrogen bond connecting B:GLU:288 and the NH group in the other tetrazole ring at a distance of 2.61 Å, in addition to some other bonds, as shown in Fig. 8 and Table 4.

Table 4. Molecular docking results for some compounds

Comp No.	Affinity (Kcal/mol)	RMSD l.b. (A°)	RMSD u.b. (A°)	Distance (A°)	Main residue	Type of Interaction
N6	-10.4	5.193	10.388	2.82795	A:THR94:OG1 - :UNK1:N	Conventional Hydrogen Bond
				2.51301	:UNK1:H - A:SER93:OG	Conventional Hydrogen Bond
				3.07441	:UNK1:H - A:THR94:OG1	Conventional Hydrogen Bond
				3.64652	A:LYS99:NZ - :UNK1	Pi-Cation
				4.12535	A:GLU194:OE1 - :UNK1	Pi-Anion

				3.58498	A:GLU194:OE2 - :UNK1	Pi-Anion
				2.96715	A:ARG120:O - :UNK1	Pi-Lone Pair
				4.66463	A:TRP127 - :UNK1	Pi-Pi T-shaped
				4.94979	A:TRP127 - :UNK1	Pi-Pi T-shaped
				5.21369	:UNK1 - A:ARG120	Pi-Alkyl
				4.3998	:UNK1 - A:ARG120	Pi-Alkyl
				5.24101	:UNK1 - A:LEU192	Pi-Alkyl
				5.02981	:UNK1 - A:LEU96	Pi-Alkyl
				5.21063	:UNK1 - A:LYS99	Pi-Alkyl
				2.82795	:UNK1 - A:LYS100	Pi-Alkyl
N10	-9.9	4.721	8.679	3.34695	B:ARG338:NH1 - :UNK1:O	Conventional Hydrogen Bond
				2.38998	:UNK1:H - B:GLY114:O	Conventional Hydrogen Bond
				2.60956	:UNK1:H - B:GLU288:OE2	Conventional Hydrogen Bond
				3.48372	B:GLY162:CA - :UNK1:N	Carbon Hydrogen Bond
				3.76267	B:LYS238:CE - :UNK1:N	Carbon Hydrogen Bond
				4.46889	B:ARG338:NH2 - :UNK1	Pi-Cation
				4.80628	B:GLU288:OE2 - :UNK1	Pi-Anion
				4.01018	B:PHE84 - :UNK1	Pi-Pi Stacked

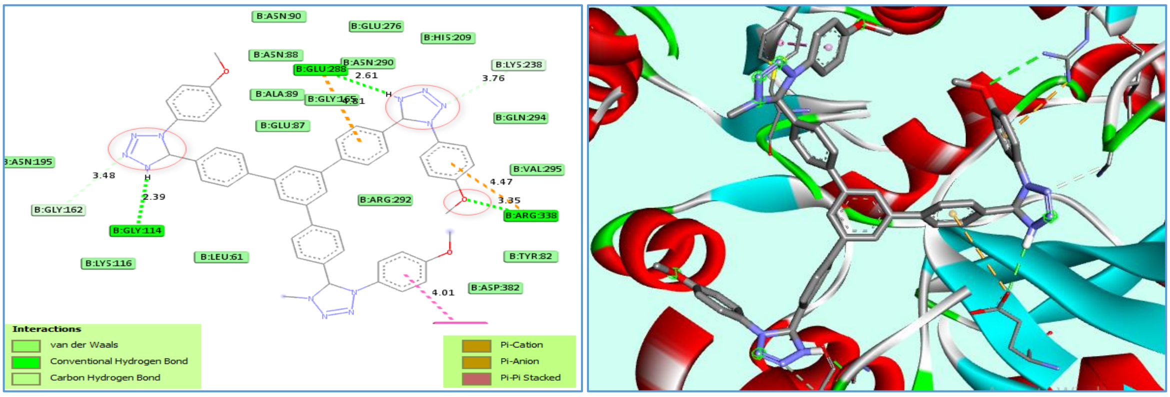

Fig. 8. 2D and 3D representation of N_{10} with the binding site of the protein (PDB:ID:3jzf)

3.6. Study of liquid crystal phases. Based on the characteristic physical and chemical properties of the prepared organic compounds, the appearance of liquid crystal phases was studied using a polarized light microscope (POM) equipped with an electric heater, where the thermal transitions of the compounds were monitored during the heating process, and the stability of the characterized phases was analyzed [33, 34].

Compound N_6 showed a clear transition from the solid crystalline state (Cr) to the fishy phase (SC) and then to the nematic phase (N) with increasing temperatures (Cr → SC → N → I.T.). During heating, the transitions were observed at 116°C, 133°C, and 147°C, respectively; this transition sequence reflects a rigid mesogenic structure that allows the transition to organized phases (SC and N) before reaching the actual liquid phase (Fig. 9).

Compound N_8 recorded a transition to the nematic phase (N) only upon heating (Cr → N → I.T) at temperatures of 159°C and 187°C and also showed a nematic transition upon cooling at 176°C and 19°C. These results indicate that the nematic phase of the compound is stable during heating and cooling, indicating enantiotropic behavior (Fig. 10).

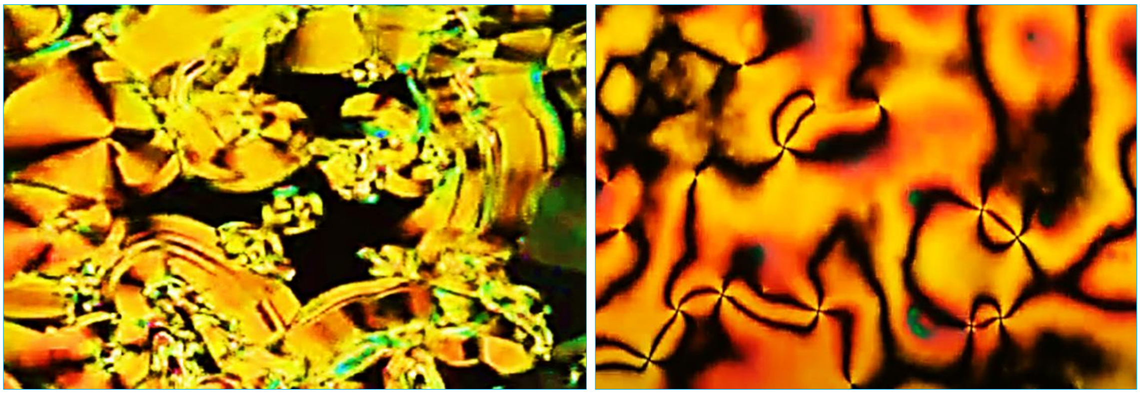

Fig. 9. SC and nematic phase of compound N_6

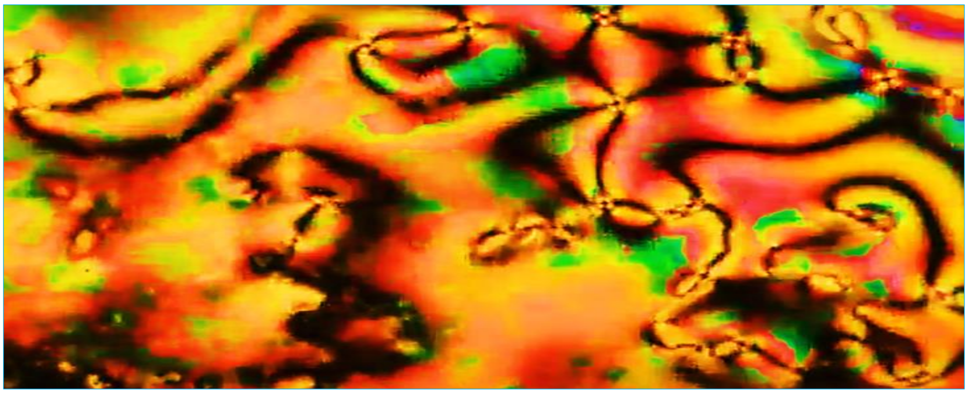

Fig.10. Nematic phase of compound N_8

4. Conclusions

Heterocyclic pentameric rings are often produced when Schiff base derivatives are combined with materials with appropriate functional groups. According to the results of bioassays, the majority of the synthesized compounds exhibit antibacterial activity. At a dosage of 0.1 mg/mL and an inhibition diameter of 1.7 cm, compound N6 showed the maximum inhibition, exceeding the efficacy of the antibiotic. With an inhibition diameter of 3.6 cm at a dosage of 0.1 mg/mL, compound N10 showed the strongest inhibitory effect against E. coli, exceeding the antibiotic in all experiments. The bacterial growth was inhibited. Many of the synthesized compounds were also shown to be stable to neodymium nanolaser light. Molecular modeling was performed using the AUTODOCK software package for N6 against S. aureus and N6 against E. coli. It appears that the tetrazole is linked via the NH group to amino acid residue B:GLY:114, forming hydrogen bonds with an affinity value of -9.9 kcal/mol and conformational values RMSD.i.b (4.721) and RMSD.u.b (8.679). Upon examination of the liquid crystals, smectic and nematic phases were detected. Spectroscopic and physical studies confirmed the exact structures of the produced compounds.

References

1. Cabrele C., Reiser O. The modern face of synthetic heterocyclic chemistry. *The Journal of Organic Chemistry*, 2016, **Vol**. **(81)21**, p. 10109-10125. DOI: 10.1021/acs.joc.6b02034
2. Morjan R.Y., Al-Attar N.H., Abu-Teim O.S., Ulrich M., Awadallah A.M., Mkadmh A.M., Elmanama A.A., Raftery J., Abu-Awwad F.M., Yaseen Z.J., Elqidrea A.F., Gardiner J.M. Synthesis, antibacterial, and QSAR evaluation of 5-oxo and 5-thio derivatives of 1, 4-disubstituted tetrazoles. *Bioorganic & medicinal chemistry letters*, 2015, **Vol**. **25(18)**, p. 4024-4028. DOI: 10.1016/j.bmcl.2015.04.070
3. Bommagani S., Penthala N.R., Balasubramaniam M., Kuravi S., Caldas-Lopes E., Guzman M.L., Balusu R., Crooks P.A. A novel tetrazole analogue of resveratrol is a potent anticancer agent. *Bioorganic & medicinal chemistry letters*, 2019, **Vol. 29(2)**, p. 172-178. DOI: 10.1016/j.bmcl.2018.12.006
4. Benson F.R. The chemistry of the tetrazoles. *Chemical Reviews*, 1947, **Vol. 41(1),** p. 1-61. DOI: 10.1021/cr60128a001
5. Gao H., Shreeve J.N.M. Azole-based energetic salts. *Chemical reviews*, 2011, **Vol**. **111(11)**, p. 7377-7436. DOI: 10.1021/cr200039c
6. Malik M.A., Wani M.Y., Al-Thabaiti S.A., Shiekh R.A. Tetrazoles as carboxylic acid isosteres: chemistry and biology. *Journal of Inclusion Phenomena and Macrocyclic Chemistry*, 2014, **Vol**. 78, p. 15-37. DOI: 10.1007/s10847-013-0334-x
7. Wittenberger S.J. Recent developments in tetrazole chemistry. A review. *Organic Preparations and Procedures International*, 1994, **Vol**. **26(5)**, p. 499-531. DOI: 10.1080/00304949409458050
8. Manzoor S., Yin X., Zhang J.G. Nitro-tetrazole based high performing explosives: Recent overview of synthesis and energetic properties. *Defence Technology*, 2021, **Vol**. **17(6)**, p. 1995-2010. DOI: 10.1016/j.dt.2021.02.002
9. Abdul Wahed Abdul S.T., Mohammed Jwher S., Jamil Nadhem S. Preparation, Characterisation and Study of the Molecular Docking of Some Derivatives of the Tetrazole Ring and Evaluation of their Biological Activity. *World of Medicine: Journal of Biomedical Sciences*, 2024, **Vol**. **1(7)**, p. 15-23.
10. Alasadi Y.K., Jumaa F.H., Dalaf A.H., Shawkat S.M., Mukhlif M.G. Synthesis, Characterization, and Molecular Docking of New Tetrazole Derivatives as Promising Anticancer Agents. *Journal of Pharmaceutical Negative Results*, 2022, Vol. 13(3), p. 513-522. DOI: 10.47750/pnr.2022.13.03.079
11. Dalal M.J., Mekky A.H. Synthesis, Characterization and Antioxidant Evaluation of Some Tetrazole Derivatives. *Indonesian Journal of chemistry*, 2022, **Vol. 22(6)**, p. 1596-1604. DOI: 10.22146/ijc.74912

12. Muhammad F.M., Khairallah B.A., Albadrany K.A. Synthesis, characterization and antibacterial evaluation of novel 1, 3-oxazepine derivatives using a cycloaddition approach. *Journal of Angiotherapy*, 2024, **Vol**. **8(3)**, p. 1-9. DOI: 10.25163/angiotherapy.839506
13. Al-Joboury W.M., Al-Badrany K.A., Asli N.J. N-alkylation of substituted 2-amino benzothiazoles by 1, 4-bis (bromo methyl) benzene on mixed oxides at room temperature and study their biological activity. In *AIP Conference Proceedings*. 2022, **Vol 2394**, 040054. DOI: 10.1063/5.0123463
14. Abdullah S.H., Salih M.M., Al-Badrany A. Synthesis, Characterization and Antibacterial Evaluation of Novel Thiazolidine Derivatives. *Journal of Angiotherapy*, 2024, **Vol. 3(3)**, p. 1-9. DOI: 10.25163/angiotherapy.839501
15. Alrashidy A.A.M., Hashem O.A., ALBadrany K.A.A. Spectrophotometric Determination of Vitamin C Using Indirect Oxidation with a New Organic Dye. *Journal of Angiotherapy*, 2024, **Vol. 8(2)**, p. 1-7. DOI: 10.25163/angiotherapy.829499
16. Al-Joboury N.A., Al-Badrany K.A., Hamed A.S., Aljoboury W.M. Synthesis of some new thiazepine compounds derived from chalcones and evaluation there biochemical and biological activity. *Biochemical & Cellular Archives*, 2019, **Vol. 19(2)**, p.4545-4554. DOI: 10.35124/bca.2019.19.2.4545
17. Dalaf A.H., Jumaa F.H., Yass I.A. Synthesis, characterization, biological evaluation, molecular docking, assess laser efficacy, thermal performance and optical stability study for new derivatives of bis-1, 3-oxazepene and 1, 3-diazepine. In *AIP Conference Proceedings*, 2022, **Vol. 2394**, 040037. DOI: 10.1063/5.0121213
18. Aftan M.M., Talloh A.A., Dalaf A.H., Salih H.K. Impact para position on rho value and rate constant and study of liquid crystalline behavior of azo compounds. *Materials Today: Proceedings*, 2021, **Vol. 45(6)**, p. 5529-5534. DOI: 10.1016/j.matpr.2021.02.298
19. Faraj E.M., Jumaa F.H. Preparation, diagnostics and biological evaluation of new Schiff base and tetrazole derivatives. *Materials Today: Proceedings*, 2022, **Vol. 49(6)**, p. 3549-3557. DOI: 10.1016/j.matpr.2021.08.061
20. Aziz F.N.E.D., Juma F.H. Synthesis, Characterization, Biological Activity, Laser Effect and Molecular Docking of Tri-Imidazole-4-One Derivatives. *SAR J Med Biochem*, 2025, **Vol**. **6(1)**, p. 4-14. DOI: 10.36346/sarjmb.2025.v06i01.002
21. Najm R.S., Shannak Q.A., Dalaf A.H. Synthesis and Decoration of Aromatic Derivatives Nano Platelets by the Electric Method. *Azerbaijan Pharmaceutical and Pharmacotherapy Journal*, 2023, **Vol**. **22(2)**, p. 92-97. DOI: 10.61336/appj/22-2-22
22. Najm R.S., Al-Somaidaie G.H. Carbonation and preparation of reduced graphene oxide sheets from cellulose. In *39th PATTAYA International Conference on "Advances in Chemical, Agriculture, Biology & Environment"(PCABE-22) Pattaya (Thailand) Aug*. 2022, **Vol.** (3), p. 25-26. DOI: 10.17758/DIRPUB12.DIR0822212
23. Khurshid M.N., Jumaa F.H., Jassim S.S. Synthesis, characterization, and evaluation of the biological activity of tetrazole compounds derived from the nitrogenous base uracil. *Materials Today: Proceedings*, 2022, **Vol**. **49(8)**, p. 3630-3639. DOI: 10.1016/j.matpr.2021.08.203
24. Al-Badrani H., Ezzat N.S., Al-Jawaheri Y.S. Synthesis of oxazepino compound via electrophilic cyclization and evaluation of their biological activity. *Chemical Problems*, 2025, **Vol**. **23(3)**, p. 343-355. DOI: 10.32737/2221-8688-2025-3-343-355
25. Murad Z.A., Hamad A.S. Preparation and diagnosis of new derivatives of the tetrazole ring derived from 2-bromoisophthaladehyde and evaluation of their biological effectiveness. *Chemical Problems*, 2025, **Vol**. 23(1), p. 116-124. DOI: 10.32737/2221-8688-2025-1-116-124
26. Najm R.S., AL-Rasheed A.A., Mohammed A.S., Graba B., Saleh M.J. Synthesis, Chemical Characterization and Biological Activity Evaluation of Lamb Meat-Derived Nanocomposite. *Advanced Journal of Chemistry, Section A*, 2025, **Vol. 8(12)**, p. 1890-1903. DOI: 10.48309/AJCA.2025.524268.1849

27. Khalil S.L., Saleem N.H. Synthesis and characterization of five-membered heterocyclic compounds of tetrazole derivatives and their biological activity. *Chemical Problems*, 2025, **Vol**. **23(3)**, p. 365-374. DOI: 10.32737/2221-8688-2025-3-365-374
28. Hassan B.A., Mekky A.H. Synthesis, characterization and antibacterial activity of [1, 2, 4] triazolo [4, 3-b][1, 2, 4, 5] tetrazine derivatives. *Chemical Problems*, 2025, **Vol.** (1), p. 78-94. DOI: 10.32737/2221-8688-2025-1-78-94
29. Hassan B.A., Fadil M.H. Synthesis and Pharmaceutical Activity of Triazole Schiff Bases With Theoretical Characterization. *Chemical Problems*, 2024, **Vol. 22(3)**, p. 332-341. DOI: 10.32737/2221-8688-2024-3-332-341
30. Hassan B.A., Fadil M.H., Mekky A.H. Synthesis, characterization, and pharmaceutical activity of fused triazolothiadiazole derivatives. *Chemical Problems*, 2025, **Vol. 23(4)**, p. 465-475. DOI: 10.32737/2221-8688-2025-4-465-475
31. Dalaf A.H., Jumaa F.H., Aftana M.M., Salih H.K., Abd I.Q. Synthesis, Characterization, Biological Evaluation, and Assessment Laser Efficacy for New Derivatives of Tetrazole. In *Key Engineering Materials*, 2022, **Vol**. 911, p. 33-39. DOI: 10.4028/p-6849u0
32. Jumaa F.H., Shawkat S.M. Synthesis, assess biological activity and laser efficacy of some new bis-1, 3-oxazepene 4, 7-dione derivatives. In *AIP Conference Proceedings*, 2022, **Vol. 2394**, 040025. DOI: 10.1063/5.0121426
33. Jumaa F.H., Yass E.A., Ibrahim B.K. Synthesis, Study of Their Liquid Crystal, Laser Properties of New Binary 1, 3-Oxazepine-4, 7-dione Derivatives and Evaluation of the Antibacterial Activity of Some of Them. *Journal of Global Scientific Research*, 2023, **Vol**. **8(9)**, p. 3201-3214. DOI: 10.5281/jgsr.2023.8312720
34. Ahmed S.E., Ahmed Z.A.G., Mustafa G.S., Saleh M.J., Saleh J.N. Preparation and Characterization of New Azetidine Rings and Evaluation of Their Biological Activity. *Advanced Journal of Chemistry, Section A*, 2025, **Vol. 9(1)**, p. 146-154. DOI: 10.48309/AJCA.2026.538779.1898.